Energetics of Br−H−Br⁻ Formation from HBr Dimer Anion: An ab Initio Study

A. Rauk* and D. A. Armstrong*

Department of Chemistry, University of Calgary, Calgary, Alberta T2N 1N4, Canada

Received: March 28, 2000; In Final Form: May 19, 2000

Experimental studies have shown that the dissociative attachment of electrons to HBr monomer; viz., HBr + $e^- \rightarrow H^\bullet + Br^-$ is an endothermic process, which requires electrons of energy near the endothermicity ($\Delta E = +38$ kJ/mol). In contrast the attachment to the dimer via the reaction: $HBr{\cdot}HBr + e^- \rightleftharpoons HBr{\cdot}HBr^{\bullet-} \rightarrow H^\bullet + BrHBr^-$ proceeds readily with electrons of thermal (i.e., near zero) energy. The energetics of the reactions with both the monomer and the dimer have been studied by ab initio methods. In each case the structure of the neutral and anion species have been computed using large basis sets and diffuse orbitals at the MP2 level. Energies have been obtained at this level and at the CCSD(T) level. The initial interaction of the free electron with the molecule produces a dipole continuum state (DCS) of the anion. The DCS subsequently undergoes a transition to a bound state via an avoided crossing. On the basis of the CCSD(T) energies, the $H-Br^{\bullet-}\cdot\cdot\cdot HBr$ interaction lowers the energy for dissociation of the $H-Br^{\bullet-}$ bond to the thermal energy range. Also the decomposition of $HBr{\cdot}HBr^{\bullet-}$ to $H^\bullet$ and $BrHBr^-$ is 47 kJ/mol exergonic and the $BrHBr^-$ fragment is expected to be in a vibrationally excited state. In both the monomer and dimer anions the transition from DCS to the bound valence state is very sudden, and is marked by enormous (10-fold) changes in the dimensions of the orbitals occupied by the electron.

Introduction

The reaction of electrons with hydrogen bromide has been a subject of interest for many years. In the nineteen thirties, Eyring, Hirschfelder and Taylor[1] proposed that the dissociative attachment (DA) with HBr monomer, viz.

$$HBr + e^- \rightarrow H^\bullet + Br^- \qquad (1)$$

would be a competitive process at thermal energies. This was based on the assumption that it was an exothermic process, i.e., that the electron affinity (EA) of Br exceeded the bond dissociation enthalpy (BDE) of HBr. Subsequent studies have shown that to be untrue. The EA of Br is now known to be 324.7 kJ mol^{-1} and the BDE of HBr is 363 kJ mol^{-1},[2] which causes reaction 1 to be endothermic by 38 kJ mol^{-1}. In the last three decades the reaction has been studied extensively, along with the competing processes of vibrational excitation and electron scattering.[3−5] The threshold energy observed by beam methods, 26−37 kJ mol^{-1},[4] is somewhat below the thermochemical threshold. That feature is common to the DA processes of HF and HCl, and has been attributed to an enhanced DA rate for the higher rotational levels of the HX molecules in the vibrational ground state. Evidence for a significant threshold energy for reaction 1 has also been obtained with thermal electrons at ambient temperature in a flowing afterglow with a helium carrier gas.[6] Here the rate constants measured at 300 and 510 K indicated an apparent activation energy of 27 kJ mol^{-1}, which is consistent with the threshold of the beam results. Also the observed rate constant for reaction 1 at 300 K was relatively small, 3.3×10^{-12} cm^3 s^{-1}. This may be compared to 2.3×10^{-7} cm^3 s^{-1} for SF_6,[7] which is near to the theoretical maximum.[8]

The concentrations of HBr in the flowing afterglow experiments were relatively low. The rate of capture of electrons of thermal energy by HBr has also been measured at much higher concentrations [(0.1 to 2) $\times 10^{19}$ cm^{-3}] in radiation chemistry experiments.[9−11] The rates were much faster than would be expected from the flowing afterglow rate constant, and were second order in HBr concentration, showing that two HBr molecules were involved. That observation led to the proposal that the thermal electron capture involved an HBr·HBr dimer[10,11] viz.:

$$HBr + HBr \rightleftharpoons HBr{\cdot}HBr \qquad (2/-2)$$

$$HBr{\cdot}HBr + e^- \rightleftharpoons HBr{\cdot}HBr^{\bullet-} \qquad (3/-3)$$

$$HBr{\cdot}HBr^{\bullet-} \rightarrow H^\bullet + BrHBr^- \qquad (4)$$

In these early studies the rate of reaction 3 was followed by competing the HBr against the specific electron scavenger SF_6. More recently the second order dependence on HBr was confirmed by totally independent physical experiments, which employed the thermal electron swarm method.[12] As well as the dependence on HBr concentration, the rate constants observed were in agreement with those obtained by the competition method.

The novelty in the above mechanism lay mainly in the concept that the energy of the $Br^-\cdot\cdot\cdot HBr$ interaction in the product $BrHBr^-$ ion would cause the threshold energy for $H-Br^{\bullet-}$ dissociation to be lower in the $HBr^{\bullet-}\cdot\cdot\cdot HBr$ complex than in $HBr^{\bullet-}$ monomer. In fact for reaction 4 to compete with auto detachment in reaction −3 that threshold must be zero or very near to thermal energy. Experimental support for this first came from the observation of electron transfers from fast alkali atoms (namely Rb) to hydrogen halide clusters ($(HX)_n$) in crossed beam experiments.[13] For HF, HCl and HBr, dissociative electron attachment to form a halide ion, solvated by hydrogen

* To whom correspondence should be addressed (rauk@ucalgary.ca and armstron@ucalgary.ca).

10.1021/jp001151r CCC: $19.00
Published on Web 07/22/2000

halide (HX), viz.:

$$Rb + (HX)_n \rightarrow Rb^+ + H^\bullet + X^{-\bullet}(HX)_{n-1} \qquad (5)$$

was the major process observed. Since that work extensive studies of the reactions of slow electrons with molecules in clusters of various sizes have been made.[14,15] Among other findings, these confirmed that threshold energies of dissociative electron attachment can be lowered by the presence of solvating neutrals. However, for the HBr system the extent of lowering of the energy and the nature of the potential energy surface for the dissociation of $HBr{\cdot}HBr^{\bullet-}$ in reaction 4 remain unknown. The purpose of this investigation was to examine those aspects of the system using modern ab initio methods, employing the Gaussian-98 molecular orbital packages.[16,17]

The electronic states of the monomer $HX^{\bullet-}$ negative ions have been studied by both theoretical and experimental methods.[3−5,18−24] The energy dependences of the cross sections for electron scattering, vibrational excitation and DA in reaction 1 have served as important experimental probes, and several states are required to explain the observations. However, for present purposes we can assume that only the lowest of these, the $HX^{\bullet-}(1^2\Sigma^+)$ state, which correlates with $H^\bullet + X^-$ at infinite separation, is relevant. This is also the state involved in the process of associative detachment, the reverse of reaction 1 where an $H^\bullet$ atom reacts with a halide ion to give an electron and HX. The fact that it occurs with a near Langevin cross section in HCl[25] is consistent with $HX^{\bullet-}(1^2\Sigma^+)$ being a state with minimal or negligible barriers to dissociation.

The approach here is to employ conventional electronic structure methods to examine the electron capture process. The "state" of the system corresponding to the left-hand side of eq 1 (or (3)) is one in which the electron is not bound to the neutral, but is interacting weakly with its dipole field. This state is referred to as a dipole continuum state (DCS). The approximate description of such a state as a quasi-bound state required very diffuse functions in the basis set. The DCS correlates directly with a dipole bound state (DBS) in the event that the dipole field is large enough to bind the electron.[26,27] The first step was to compute the potential energy (PE) curves for Σ^+ ground states of HBr and $HBr^{\bullet-}$. The geometries and energies of the neutral dimer and the dimer anion state of closest geometry were then computed. To assess the change in threshold energy, the PE dependences for the stretching of the $H-Br^{\bullet-}$ bonds in the monomer and dimer systems were compared, using the energies of the neutral ground states as reference energies. Following that we considered the final dissociation to $H^\bullet$ and $BrHBr^-$, computing the equilibrium geometry and energy of the $BrHBr^-$ product. From the results one can show that the threshold energy for dissociation of $H-Br^-\cdots HBr$ into $H^\bullet + BrHBr^-$ is much lower than for the $H-Br^{\bullet-}$ dissociation to $H^\bullet + Br^-$, and in fact accessible for electrons at thermal energies.

The crucial point is of course the energy in the region of the intersection between the PE curves of the neutral (+ unbound electron) and the ionic product. From the earlier calculations on the monomer and from studies of related dimer systems[28] it was evident that the desired accuracy would require the use of large basis sets with diffuse functions, and that the calculations would have to be done at a high level. Computations on both the monomer and the dimer systems were done at MP2 and CCSD(T) levels. The latter level of course gave greater accuracy. However, it required more computational time, and to use it for all computations on the dimer systems would have been prohibitive. Therefore, the results for the PE curves of the monomer Σ^+ ground states of HBr and $HBr^{\bullet-}$ at the CCSD(T) and MP2 levels were compared, and conclusions were drawn as to where economies could be made at the MP2 level in the calculations on the larger HBr dimer system.

Computational Details

All ab initio calculations presented here were performed with the Gaussian-98 molecular orbital packages.[16,17] The geometry optimizations and vibrational frequency calculations were carried out at the MP2 level with 6-311+G(3df,2p) basis sets on Br and aug-cc-pvdz on H. Although these basis sets are already quite complete, additional diffuse functions are required for proper description of the negative ion species,[20,21,28] particularly to let the electron "escape". As in ref 28 the ones used here were four sets of s and p-type Gaussian functions with exponents 0.005625, 0.001125, 0.000225, and 0.000045. The complete set is referred to below as "the diffuse" functions. In the monomer $HBr^{\bullet-}$ these were placed on the Br atoms. In the cases of the $HBr{\cdot}HBr$ and $HBr{\cdot}HBr^{\bullet-}$ dimers, calculations were made with them on the distal H, the H-bonded H and the Br between those two. The differences between the geometries and energies derived by these three methods were negligible. Therefore, further calculations were performed with them on the H-bonded hydrogen, since this one becomes the center of the $BrHBr^-$ product ion. Identical basis set distributions were used for the neutral HBr monomer and $HBr{\cdot}HBr$ dimer. Vibrational frequencies and zero point energies (ZPEs) were computed at the MP2 level and scaled by 0.96. CCSD(T) calculations were carried out with the same basis sets.

The PE curves for the stretching of the H−Br bond were obtained by using the "Scan" procedure of Gaussian 98.[29] In the case of the monomer that was done both at the MP2 and CCSD(T) levels. However, this was not practical for the $HBr{\cdot}HBr$ and $HBr{\cdot}HBr^{\bullet-}$ dimers. Thus, single point CCSD(T) calculations were performed on the MP2 optimized geometries of $HBr{\cdot}HBr$ and $HBr{\cdot}HBr^{\bullet-}$, and on the $H^\bullet + BrHBr^-$ products. CCSD(T) calculations were also done on selected geometries in the region of the transition between the $HBr{\cdot}HBr^{\bullet-}$ DCS and the products.

Results and Discussion

HBr and $HBr^{\bullet-}$. The optimized MP2 structure of $HBr(X^1\Sigma^+)$ has an r_e value of 1.419Å which agrees well with the experimental value of 1.414 Å.[30] The ZPE and vibrational frequency were 15.6 kJ mol^{-1} and 2607 cm^{-1}, respectively. These are again in reasonable agreement with the experimental values: 15.6 kJ mol^{-1} and 2649 cm^{-1}, respectively.[31] The MP2 and CCSD(T) energies have been presented in Table 1. The BDE of HBr and EA of Br were calculated as a means of checking the reliability of thermochemical data obtained by the present methods for the bromine system, and these results are also presented in Table 1. The CCSD(T) energies give excellent agreement with experiment for the EA and are within 3 kJ mol^{-1} of the experimental value of the BDE. The MP2 results give a similar agreement on the BDE, but overestimate the EA by 9 kJ mol^{-1}.

The dependences of the potential energy (PE) of $HBr(X^1\Sigma^+)$ and $HBr^{\bullet-}(1^2\Sigma^+)$ on internuclear distance, with the energies normalized to the respective MP2 and CCSD(T) values of the neutrals at r_e, are shown in Figure 1a. The solid parabolic line is the curve for the neutral $HBr(X^1\Sigma^+)$ PE well, based on the CCSD(T) energies. The MP2 curve, which has not been shown, is virtually identical with the minimum shifted to a slightly smaller (0.003 Å) internuclear distance. Both the MP2 and

TABLE 1: Energies of HBr Species[a] (in Hartrees) and Electron Affinity and Bond Dissociation Enthalpy (in kJ mol^{-1})

	(aug-cc-pvdz) MP2/CCSD(T)	(6-311+G(3df,2p) + diff functions) MP2	(6-311+G(3df,2p) + diff functions) CCSD(T)	exp[b]
H•	−0.49981			
Br•		−2572.66853	−2572.68065	
Br⁻		−2572.79532	−2572.80393	
EA		333	323.7	324.7
		Br(6-311+G(3df,2p) + diff functions) and H(aug-cc-pvdz)) MP2	Br(6-311+G(3df,2p) + diff functions) and H(aug-cc-pvdz)) CCSD(T)	
HBr		−2573.31032	−2573.32339	
BDE		359	360	363
HBr•⁻		−2573.31027	−2573.32334	
vertical attachment energy		0.13	0.13	

[a] For HBr and HBr•⁻ on the geometry computed with (6-311+G(3df,2p) basis sets + diff orbitals on bromine and (aug-cc-pvdz)) on hydrogen. [b] From ref 2.

CCSD(T) PE curves for the neutral were insensitive to the presence of the diffuse functions. However, the dependence of the PE of HBr•⁻($1^2\Sigma^+$) on r is much more complex, being very sensitive to the presence of diffuse functions and showing some differences between MP2 and CCSD(T) levels. The filled points refer to MP2 and open ones to CCSD(T) energies. Triangles, squares and circles refer to calculations carried out with no, one and four diffuse functions, respectively. It is convenient to discuss the regions lying to the right of the neutral PE well and within the neutral PE well, and the cross over region separately.

At r values in excess of 1.70 Å the HBr•⁻($1^2\Sigma^+$) PE curve lies well below that of the neutral, and, as shown by a comparison of the circles, squares and triangles, it is insensitive to the presence of the diffuse orbitals. As discussed previously for HBr[23] and the related HCl system[19−21] this curve correlates with H + Br⁻ at infinite r and corresponds to a well-defined bound state or valence state. Within the PE well of the neutral the PE curve of the lowest HBr•⁻ state, *computed in the absence of the diffuse functions*, is contiguous with the points lying to the right of the well and must correlate with the same bound state, in which the electron occupies the antibonding orbital of the HBr bond, σ^*_{HBr}. This "valence" state is repulsive within the well of the neutral. Comparison of the open and closed points shows that for r between 1.4 and 2.2 Å the MP2 energy for it agrees with the CCSD(T) energy to within ≤4 kJ mol^{-1}. However, the heavy line drawn through the points is based on the CCSD(T) energies, which are regarded as more accurate.

As illustrated by the squares, which show the energies calculated with only the tightest diffuse function (i.e., the one with the largest exponent) and the circles, showing the energies with all diffuse functions, the energies of HBr•⁻ within the PE well of the neutral fall as diffuse functions are added. In fact in the presence of the full set of diffuse functions the PE dependence parallels that of the neutral for both the MP2 and CCSD(T) calculations and, in effect, describes the situation where the electron has escaped. Also the MP2 calculation gave the same r_e, vibrational frequency and ZPE for HBr•⁻ as for HBr, as expected. The anion energy at r_e is 0.05 mhartrees higher than for the neutral at both the MP2 and CCSD(T) levels. The differences would be zero in the limit of a plane wave description of the electron.

The present observations parallel the results reported for the related HCl system.[19−21] Also a dependence of the energy of HBr•⁻($1^2\Sigma^+$) on the "tightness" of the basis sets was reported in the work of Chapman et al.[23] The presence of the diffuse functions apparently allows the electron in the energy continuum to interact with the molecular dipolar field, and the electron occupies an orbital as diffuse as the basis set permits,[20,21] i.e.,

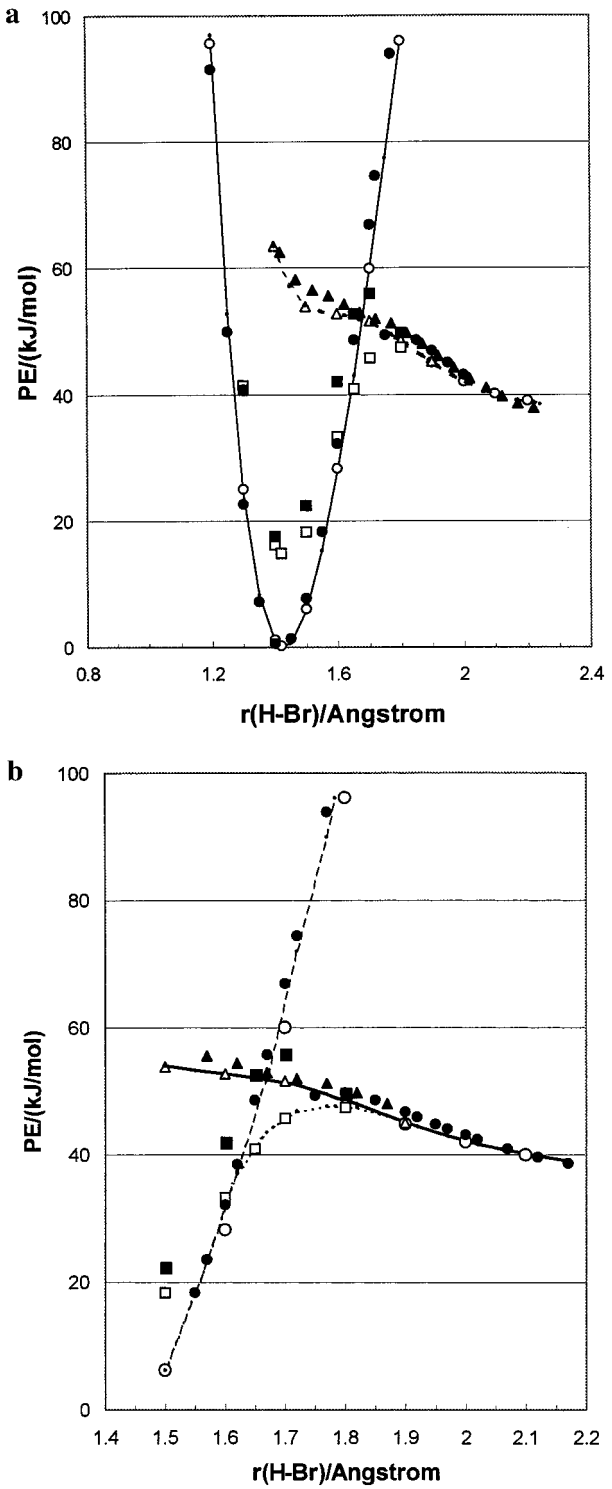

Figure 1. (a) Potential energy versus internuclear distance plots for the lowest energy states of: (a) HBr at the CCSD(T) level (thin parabolic line), and (b) HBr•⁻ from MP2 (filled symbols) and CCSD(T) (open symbols) level calculations. Energies are normalized to the respective MP2 and CCSD(T) values of the neutral at r_e. Triangles, squares and circles refer to calculations carried out with no, one and four diffuse functions, respectively. (b) Potential energy versus internuclear distance plot for HBr•⁻ in the region of the transition between the dipole continuum state (- - -) and the bound state (solid line). Symbols as in Figure 1a.

an approximation of the DCS. Without the diffuse functions one sees primarily the bound state, where the electron occupies a molecular orbital. The difference between the two is readily seen from the "electronic spatial extent" given in the Gaussian calculations. This falls from about 18 000 Å^2 with the full set of basis functions to 1000 Å^2 with none. Since the 6-311+G(3df,2p) and aug-cc-pvdz basis sets used here already provide relatively large orbitals, it is possible that the calculations with no diffuse functions still include a minor component of the dipole state character. Thus, the actual energy of the bound state in the region of the neutral PE well may be higher than shown by the triangles. We did not explore that point. However, the absence of an effect of the diffuse functions at $r > 1.8$ Å in Figure 1a indicates that beyond that H−Br distance the lowest state is the bound state. The heavy dashed line is drawn through the CCSD(T) points, and represents the best estimate of the bound state PE curve from the present study.

The region where the anion bound state curve crosses the right-hand side of the PE curve of the neutral is shown in Figure 1b on an expanded scale. The triangular points, showing energies from calculations with no diffuse functions, pass smoothly across, the solid line being drawn through the CCSD(T) points. However, energies computed with basis sets having one or more of the diffuse functions exhibit anomalies. The most obvious was the tendency for those with the complete set of four diffuse functions to converge on the "dipole continuum state" (DCS). This is shown by the open and filled circles lying above the bound state line to the right of the crossing (see also Figure 1a). That tendency was particularly evident in "scan" calculations where r was increased. Scans with decreasing r or single point calculations usually enabled one to come closer to the crossing, but very close to the crossing usually led to energies on the upper curve or, in some instances, failure of the SCF procedure to converge. These anomalies appear to arise from the failure of the present methods, which employ a single determinantal reference configuration (the UHF solution) to properly track the transition between the DCS and the bound state, which may be viewed as a narrowly avoided crossing of states with very dissimilar characters. As shown by the squares, the behavior with the single tightest diffuse function was considerably better. In fact the CCSD(T) energies gave an apparently smooth transition from the DCS to the bound state on the right side of the neutral PE well. These computations with the tightest diffuse function correspond to a situation in which the electron is permitted to partially escape, and provide a prediction of the high energy limit of the lowest state in the region of the avoided crossing. The MP2 points in general followed the CCSD(T) results. However, they tended to lie a few kJ mol^{-1} higher in energy, and with one diffuse function do not track the transition region as well.

The main objectives of this part of the present study were to find the energy profile of the lowest state of HBr$^{\bullet-}$ and to determine to what extent the more economical MP2 calculations could be used for the larger dimer system. The heavy solid line in Figure 2 is a composite curve based on the CCSD(T) energies. Energies from calculations with one diffuse function were used in the region of the crossing and from those with the set of four diffuse functions everywhere else. The actual points are reproduced by open squares and circles, respectively. For comparison, the filled circles show the energies derived from the MP2 level calculations with four diffuse functions. The CCSD(T) results in Figure 2 go beyond the r value of Figure 1a,b, and the CCSD(T) asymptotic value at infinite separation, 52.9 kJ mol^{-1}, has been shown by crosses. This agrees well

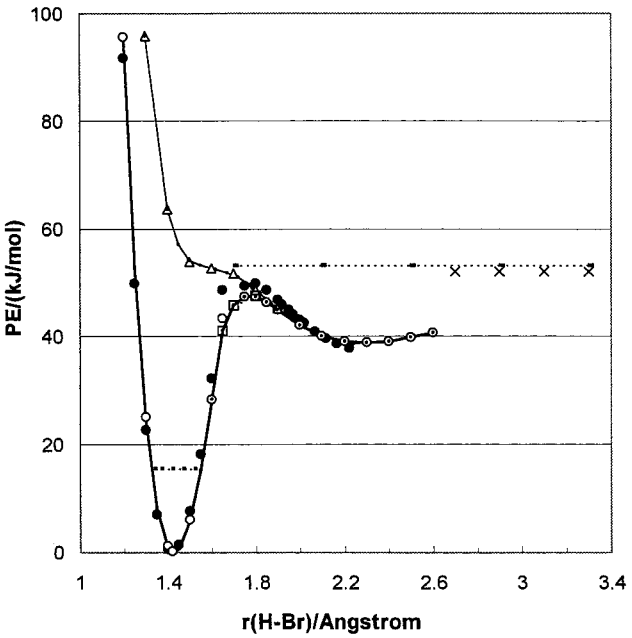

Figure 2. PE curve for lowest energy state of HBr$^{\bullet-}$ (heavy solid line). Thin line shows the repulsive bound state. Symbols as in Figure 1a. Horizontal dashed line and crosses near 50 kJ mol^{-1} show the experimental and CCSD(T) dissociation energies, respectively, at infinite r(H−Br). Dashed line at 15.6 kJ mol^{-1}: ZPE of neutral.

with the experimental value shown by the dashed line, 54.2 kJ mol^{-1}. The MP2 asymptotic value (41.1 kJ mol^{-1}) has not been shown. The much poorer agreement with experiment reflects the higher EA of Br calculated by that procedure.

It is important to note that the curve obtained without diffuse functions (the thinner line) crosses into the PE well of neutral HBr($X^1\Sigma^+$) at energies below the energy of H$^\bullet$ + Br$^-$ at infinite separation. This agrees with the calculations of Chapman et al.[23] for HBr and with the work of others on the related HCl system.[19−21] It is also indicates that there is no barrier to reaction 1 or to the reverse process, which lies above the asymptotic energy. That feature is consistent with the threshold in beam experiments being slightly lower than the thermodynamic values, as discussed above. Another important feature of the CCSD(T) data is the shallow minimum at 2.3 Å (The MP2 curve also shows a minimum, but at ∼2.4 Å). This is due to the weakly bound valence state arising from Br$^-$ to H atom-ion induced dipole binding. The above r_e value agrees with 2.25 Å reported in the study of Chapman et al.[23]

The preceding discussion of the HBr monomer indicates that CCSD(T) calculations are required to obtain meaningful energies in the region of the crossing (r = 1.6−1.7Å). However, the MP2 calculations reproduce the CCSD(T) energies to within a few kJ mol^{-1}, both in the PE well of the neutral and in the region just beyond the barrier from 1.7 to 2.0 Å. Therefore, for the dimer (see below) one may anticipate that CCSD(T) calculations will again be required in the region of the crossing. However, MP2 calculations should be useful at H−Br distances in the regions where agreement of the two methods was noted above.

HBr·HBr, HBr·HBr$^{\bullet-}$ and Br−H−Br$^-$. The MP2 optimized geometry of the neutral dimer obtained with the 6-311+G(3df,2p) basis set on Br and aug-cc-pvdz on H, plus the diffuse orbitals on the H-bonding H atom, is shown in Figure 3. The calculated Br−Br distance was 4.12 Å, which may be compared with 4.14 Å obtained by experiment for the global minimum of the neutral HBr.DBr dimer.[32] Other parameters

TABLE 2: MP2 Vibrational Frequencies in cm^{-1}

	atom numbering scheme:[a] H_2—Br_1—H_3—Br_4					
HBr−HBr	1−2 str	3−4 str	1−3−4 bend	sym rot.	unsym rot.	HBr−HBr str
neutral	2598	2551	199	270	90	47
	2708[b]	2674[b]	205[b]	288[b]	111[b]	48[b]
	2555[c]	2496[c]				
anion						
DCS state	2597	2550	198	270	89	47
valence state	asym str	sym str	1−3−4 bend	1−3−4 bend	H2 wag	H2 str
	761	202	685	685	6	114
Br−H−Br⁻	asym str	sym str	1−3−4 bend	1−3−4 bend		
	770	203	684	684		
	837[d]	200[d]				
	731[e]	188[e]				
	728[f]					

[a] The subscript numbers are used to identify atoms involved in specific vibrations. [b] Calculated in ref 33. [c] Experimental in Ar matrix from ref 34. [d] Calculated in ref 36. [e] Anharmonic frequency calculated in ref 37. [f] Experimental in Ar matrix from ref 38.

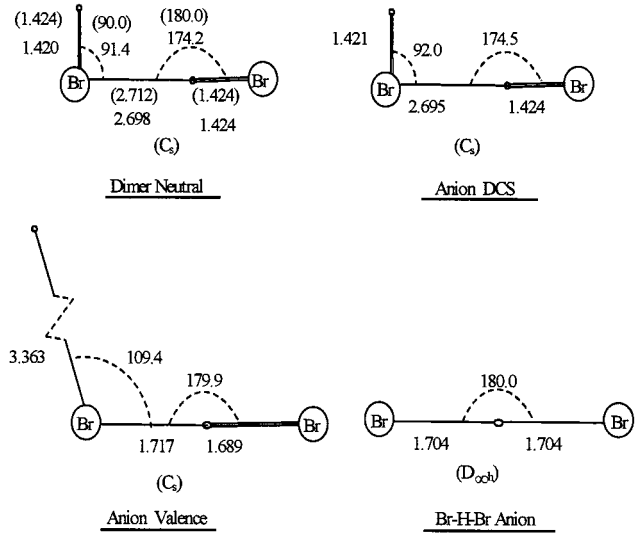

Figure 3. Structures: Large open circles Br, Small ones H. Angles in degrees, bond lengths in Å. Data in parentheses on Neutral Dimer are from ref 32.

from that study are shown in parentheses on the neutral structure, and the agreement is satisfactory. An earlier calculation by Latajka and Scheiner,[33] also at the MP2 level but with different basis sets, gave a Br−Br distance of 4.17 Å and a value of the Br−H−Br angle similar to that in Figure 3. The agreement with their other geometric parameters is not as good. However, as shown in Table 2, their frequencies are similar to those calculated here. The present stretching frequencies are in reasonable agreement with the values derived from a study of the dimer in an argon matrix.[34]

Optimization of the above structure with an electron added and the same basis sets, gave an anion with the structure shown in Figure 3 and the MP2 frequencies in Table 2. The MP2 and CCSD(T) electronic energies, ZPEs and other relevant energies for it are listed in Table 3. Comparisons of the geometry and frequencies of the anion with those of the neutral dimer shows that they are effectively identical. As in the case of the monomer, that is expected if the electron is unbound and this initial dimer anion state is a DCS. Here one should note that the HBr dimer dipole moment from the present MP2 results is 1.72 D, which is considerably less than the critical value of 2.2 D required for DBS formation.[26] In this respect HBr·HBr differs from HF·HF which has a dipole moment of ∼3.2 and forms a DBS.[28,35] The fact that at the CCSD(T) level with all diffuse functions the ΔE value for electron attachment to HBr·HBr (see the penultimate column of Table 3) is small and negative is consistent with the DCS state. Again one would expect it to be zero in the limit of a plane wave description of the electron.

When an electron was added to the neutral dimer and it was optimized *without the diffuse orbitals*, *a structure of much lower energy was obtained*. To make the system comparable to the neutral dimer and DCS, this was reoptimized with the diffuse orbitals reinstated on the H-bonded H atom (atom 3 of the scheme in Table 2). This led to only minor changes in the geometry and energy. That optimized geometry is shown in Figure 3, and the frequencies and energy for it in Tables 2 and 3, respectively. Examination of the structure and frequencies of this species suggested that it was a "valence" structure consisting of an H atom bound by ion−dipole-induced forces in the field of a Br−H−Br⁻ anion. In other words it is the analogue of the valence structure that produces the minimum at 2.3 Å in Figure 2. The optimized structure of Br−H−Br⁻ with the same basis sets, including diffuse orbitals on the H, was also calculated. The structure, frequencies and energy are presented in Figure 3 and Tables 2 and 3, respectively. The correspondence of the asymmetric and symmetric stretch frequencies and the Br−H−Br geometry in this and the valence structure is quite apparent. The weak frequencies in the valence anion are associated with the Br−H stretch and in plane wag of the loosely bound H atom. The binding energy for it is only about 1 kJ mol^{-1} (see below). The present frequencies of the Br−H−Br⁻ anion are compared with the literature data[36−38] in Table 2. It may be noted that the vibrations of this species are strongly anharmonic,[37,38] and the frequencies show a dependence on the level of calculation.[37] *Also, with allowance for anharmonicity, the Br−H distances are estimated to be 1.726* Å, *slightly longer than those in Figure 3.* However, the differences between the present frequencies and those of ref 37 are not judged to be enough to cause serious errors in the calculation of ZPEs and other energies. From the present CCSD(T) energies and ZPE values in Tables 1 and 3 the value of the binding energy of HBr to the Br⁻ anion is 86.8 kJ mol^{-1} at 0 K and 90.8 kJ mol^{-1} with correction to 300 K. The latter is close to the experimental value of 87.4 kJ mol^{-1} at 300 K.[39]

Effect of the HBr$^{\bullet-}$- -HBr Interaction on the Threshold for Dissociative Capture. The MP2 potential energy profile for the stretching of the terminal H−Br$^{\bullet-}$ bond in the DCS anion (i.e., the stretching of $r(H_2-Br_1)$) was calculated by the Gaussian 98 "Scan" procedure with the geometry of the $Br_1-H_3-Br_4$ fragment held constant. The same procedure was followed for the neutral dimer. The geometries of the $Br_1-H_3-Br_4$ fragments in these calculations were kept linear. This causes only small increases of about 0.02 mhartrees in the energies of the neutral and the DCS (Table 3), and the simplification is worthwhile.

TABLE 3: Electronic Energies (in Hartrees)[a] and ZPEs and Energies (in kJ mol^{-1}) of HBr−HBr and Br−H−Br$^-$ Species

	electronic energies				
	MP2	CCSD(T)	ZPE	$\Delta E^{b,c}$	est of vibr excit[c]
HBr−HBr					
neutral	−5146.624020	−5146.649553 (−5146.649535)[d]	34.4		
anion					
DCS state	−5146.623983	−5146.649551 (−5146.649534)[d]	34.4	0.005	
valence state	−5146.641953	−5146.660107	14.7	−47.4	
H$^\bullet$ + Br−H−Br$^-$					
Br−H−Br$^-$ (DCS geom)	−5146.628093	−5146.648726	14.0	−18.4	28
Br−H−Br$^-$ (geom of min barrier)	−5146.632418	−5146.652447	14.0	−28.0	19
Br−H−Br$^-$ (equilib geom)	−5146.641726	−5146.659583	14.0	−46.7	0
Br−H−Br$^-$					
equilib geom	−5146.141916	−5146.159773	14.0		

[a] Basis sets for optimized geometry and energies: (6-311+G(3df,2p) on bromines and (aug-cc-pvdz)) on hydrogens, plus diffuse orbitals on H_3. [b] In kJ mol^{-1} relative to optimized ground-state neutral dimer and corrected for ZPEs. [c] From CCSD(T) energies. [d] For $Br_1-H_3-Br_4$ collinear.

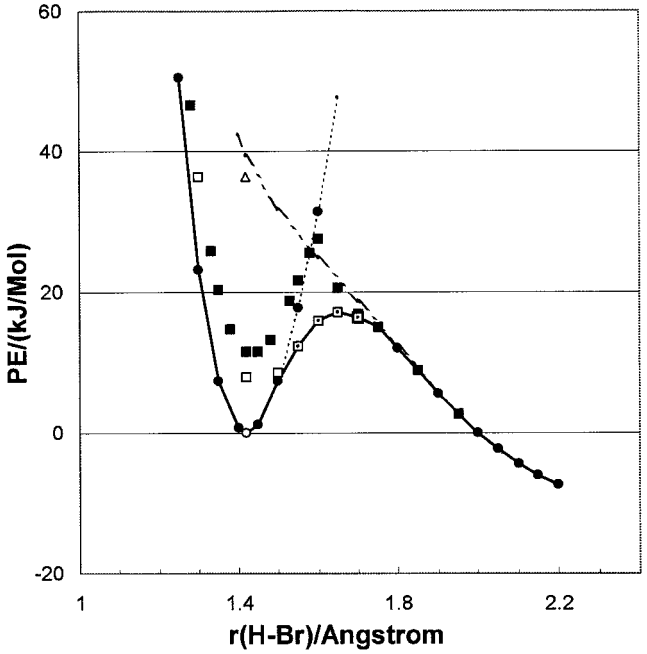

Figure 4. Potential energy versus internuclear distance plots for stretching the distal Br−H bond in the HBr dimer neutral (dashed parabolic curve) and anion (Symbols). Based on MP2 and CCSD(T) energies. Anion energies are normalized to the respective MP2 and CCSD(T) values of the neutral at r_e, and the symbols have the same significance as in Figure 1a. Solid line: lowest energy state; heavy dashed line: bound state.

The results have been plotted in Figure 4 with all energies relative to the energy of the optimized geometry of the neutral taken as zero. As in previous figures open symbols refer to CCSD(T) energies and filled ones to MP2. Likewise triangles, squares and circles refer to no diffuse functions, one and four, respectively. The thin dashed line represents the curve of the neutral calculated at the MP2 level, and the heavy dashed line the MP2 energies derived without diffuse functions, i.e., the energies most closely representing the bound state. The effects of diffuse functions are similar to those observed with the monomer, and again the CCSD(T) energies with one diffuse function pass smoothly over the crossing region. The heavy solid line is a composite curve, based on the CCSD(T) energies with one diffuse function in the crossing region, and the MP2 energies with four diffuse functions elsewhere. As in the case of the monomer, in the region below 1.5 Å the r(H−Br) PE dependence of the DCS anion merges with that of the neutral. Also, beyond ∼1.70 Å the energies become insensitive to the presence of the diffuse functions.

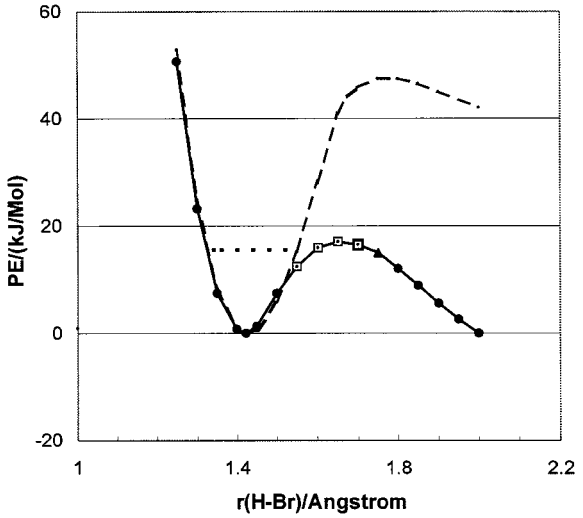

Figure 5. Comparison of threshold energies for dissociation of the H−Br bond in the HBr$^{\bullet-}$ monomer (line with long dashes) and HBr·HBr$^{\bullet-}$ dimer (solid line with symbols). The line of short dashes is the ZPE level for the HBr vibration.

Figure 5 shows a comparison of the PE dependences for the stretching of the H−Br bond in the monomer anion and of the distal H−Br in the dimer DCS anion. The barrier to dissociation is reduced by 36 kJ mol^{-1}, and is clearly in the thermal energy range near the ZPE of the HBr stretch. This is true for the present case where the geometry of the Br−H−Br$^-$ negative ion fragment does not relax from the equilibrium geometry of the DCS. That geometry actually corresponds to a vibrationally excited state of that fragment in the H$^\bullet$···BrHBr$^-$ product. If relaxation accompanied the H−Br stretch, the barrier energy should be further reduced.

Attempts to find an unambiguous transition state between the DCS and the H$^\bullet$···BrHBr$^-$ valence state by the methods normally used in the Gaussian programs were thwarted by the tendency of the calculations to converge on the DCS state (i.e., eject the electron), which was mentioned above. However, a more simplistic approach can be made. Obviously, the Br$^-$·HBr interaction should be increased and the barrier lowered by bringing the "solvating" HBr closer to the Br of the dissociating pair. Because the HBr···HBr potential in the dimer is quite soft, as indicated by the low HBr···HBr stretching frequency in Table 2, this does not require a large expenditure of energy. Calculations were therefore done for the PE dependences of the H_2-Br_1 dissociation as a function of the Br_1-H_3 distance. Figure 6 shows the results of such a calculation for $r(Br_1-H_3)$ reduced from 2.695 Å in the optimized DCS geometry to 2.4 Å. All

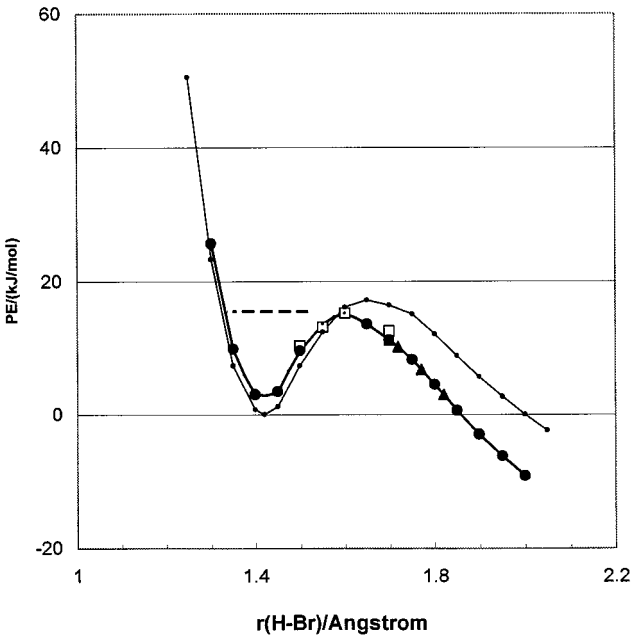

Figure 6. Comparison of threshold energies for dissociation of the H−Br bond in the HBr·HBr•⁻ dimer with $r(H_3-Br_4)$ fixed at 1.424 and $r(Br_1-H_3) = 2.695$ Å (solid line with dots) and = 2.4 (solid line with symbols). The line of dashes is the ZPE level for the H−Br bond.

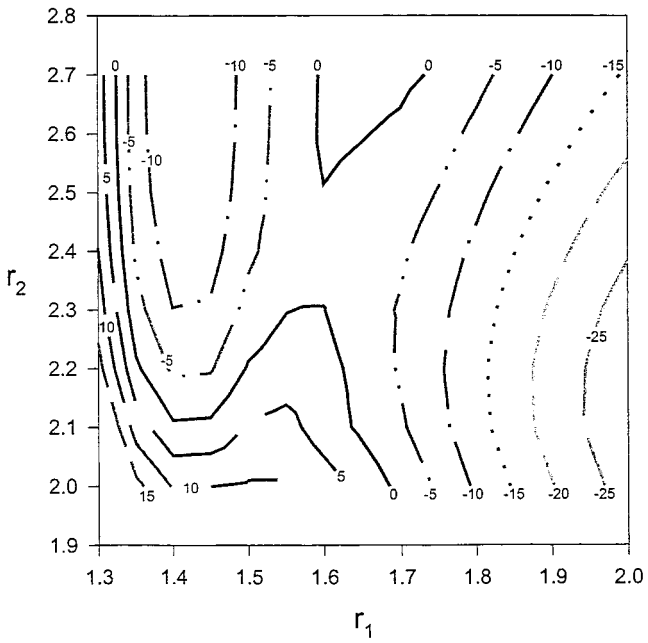

Figure 7. Potential energy surface for the HBr·HBr•⁻ anion as a function of $r_2(=r(Br_1-H_3))$ and $r_1(=r(H_2-Br_1))$. The value of $r(H_3-Br_4)$ was fixed at 1.424 Å, and the $H_2-Br_1-H_3$ and $Br_1-H_3-Br_4$ angles were respectively 91.5 and 180 degrees, respectively. The zero of energy is the ZPE level of the H−Br bond. The lowest barrier to dissociation of H_2 from Br_1 is in the region of r_2 between 2.3 and 2.5Å.

energies are relative to the energy of the optimized neutral dimer. The line with solid dots is the corresponding curve from Figure 5 for $r(Br_1-H_3) = 2.695$ Å. As expected, the barrier to dissociation is seen to be narrowed and to be reduced. Significant is the fact that it is now at or below the ZPE level for the H−Br stretching vibration of the terminal H atom in the DCS, which is shown as a horizontal dashed line.

The results of similar calculations at a series of Br_1-H_3 distance have been presented in the form of a PE surface in Figure 7. $r(Br_1-H_2)$ is the abscissa and is referred to as r_1, while $r(Br_1-H_3)$ is the ordinate, r_2. A value of 15.6 kJ mol^{-1} has been subtracted from all energies, which means that the ZPE level for the H−Br stretching vibration of the terminal H atom in the DCS is now the zero on the PE scale. For values of r_2 greater than 2.1 Å the PE first rises as r_1 increases from the r_e value of 1.421 Å, and then falls. However, in the region $2.3 < r_2 < 2.5$ it is always negative, i.e., below the ZPE value. Thus, the HBr·HBr•⁻ DCS is unstable with respect to formation of the H• + BrHBr⁻ valence state. Here it may be noted that the present calculations do not allow for simultaneous lengthening in $r(H_3-Br_4)$, which could cause further lowering of the barrier.

Energetics of the H•+BrHBr⁻ Formation. The calculations of these quantities are based on the CCSD(T) energies and the ZPEs in Table 3 and they are for 0 K. The energy change in reaction 6 is only 0.7 kJ mol^{-1},

$$H^{\bullet}\cdots BrHBr^{-} \rightarrow H^{\bullet} + BrHBr^{-} \qquad (6)$$

and the binding of the H atom is extremely weak. Thus, one can assume that the products of the DCS to bound state transition of the dimer are the separated H atom and BrHBr⁻ anion, as described by reaction 4. The difference in energy between the neutral dimer in its optimized geometry and the separated H•+ BrHBr⁻ products are given in the penultimate column of Table 3 for three geometries of the BrHBr⁻ anion. If the latter were formed with the equilibrium geometry, the overall DE would be −46.7 kJ mol^{-1}, and that should be carried off largely as kinetic energy of the H atom and some rotational excitation of the BrHBr⁻. However, from a comparison of the dimer DCS anion and BrHBr⁻ equilibrium geometries in Figure 3 it is evident that the BrHBr⁻ fragment would initially probably be highly distorted. Therefore, it seems rather likely that this fragment will be formed with excess vibrational energy. That excess energy has been calculated from the difference between the exothermicity with the equilibrium geometry and the values for the other two geometries, and is shown in the last column of Table 3. The most likely scenario would be the passage over the minimum in the barrier of Figure 7, where $r(Br_1-H_3)$ (i.e., r_2) is ∼2.4 Å and $r(H_3-Br_4) = 1.424$ Å.[40] That geometry produces an excitation energy of ∼19 kJ mol^{-1}. From the data in Table 5 of ref 37 it appears that this would require a combination of the ν_1 mode (asymmetric stretch) and several quanta of the ν_3 mode (symmetric stretch), probably ($\nu_1 + 4$ or 5 ν_3). Combinations of that type with up to 3 ν_3 have been observed. A more detailed discussion requires consideration of how much simultaneous lengthening of $r(H_3-Br_4)$ would occur in the transition state.

Conclusions

The PE profiles for the (electron + neutral) to bound state transitions for the HBr monomer and dimer anions have been estimated by using CCSD(T) and MP2 level calculations. In the region of the transition the former level is essential and only the tightest of the diffuse functions employed here could be used. The barrier found for the HBr·HBr•⁻ dimer DCS anion is expected to be an upper limit. Examination of the PE surface for that species predicts that it is unstable with respect to decomposition to H• + BrHBr⁻. This finding is in accord with experimental observations, which show that, in contrast to the electron capture reaction of the monomer, the reaction:

$$HBr\cdot HBr + e \rightarrow H^{\bullet} + BrHBr^{-} \qquad (7)$$

has a rate constant for thermal electrons similar to that of the

SF_6 reaction and close to the maximum theoretical value.[41] The binding energy of $BrHBr^-$ and other tests of energies computed at the CCSD(T) level showed that they were in excellent agreement with available experimental values. The decomposition of $HBr{\cdot}HBr^{\bullet-}$ DCS anion to $H^\bullet + BrHBr^-$ is highly exothermic and the $BrHBr^-$ species is expected to be vibrationally excited in a combination of ν_1 and ν_3 modes.

Acknowledgment. The financial support of the Natural Sciences and Engineering Research Council of Canada and the University of Calgary is gratefully acknowledged. The authors are also indebted to Dr. Dake Yu, who carried out many of the preliminary calculations on this project, and to Dr. David Cramb for assistance in the preparation of Figure 7.

References and Notes

(1) Eyring, H.; Hirschfelder, J. O.; Taylor, H. S. *J. Chem. Phys.* **1936**, *4*, 570.
(2) Lias, S. G.; Bartmess, J. E.; Liebman, J. F.; Holmes, J. L.; Levin, R. D.; Mallard, W. G. Gas-Phase Ion and Neutral Thermochemistry. *J. Phys. Chem. Ref. Data* **1988**, *17*, Suppl. No. 1.
(3) Domcke, W. *Phys. Rep.* **1991**, *208*, 97.
(4) Abouaf, R.; Teillet-Billy, D. *Chem. Phys. Lett.* **1980**, *73*, 106.
(5) Rohr, K. *J. Phys. B.* **1978**, *10*, 1849.
(6) Adams, N. G.; Smith, D.; Paulson, J. F.; Henchman, M. J.; Viggiano, A. A. *J. Chem. Phys.* **1986**, *84*, 6728.
(7) Shimamori, H.; Tatsumi, Y.; Ogawa, Y.; Sunagawa, T. *J. Chem. Phys*. **1992**, *97*, 6335.
(8) Compton, R. N.; Huebner, R. H. In *Advances in Radiation Chemistry*; Burton, M., Magee, J. L., Eds.; Wiley: New York, 1970; Vol. 2, p 281.
(9) Chen, J. D.; Armstrong, D. A. *J. Chem. Phys*. **1968**, *48*, 2310.
(10) Nagra, S. S.; Armstrong, D. A. *J. Phys*. *Chem.* **1975**, *48*, 2310; *Can. J. Chem.* **1975**, *53*, 3305.
(11) Nagra, S. S.; Armstrong, D. A. *Can. J. Chem.* **1976**, *54*, 3580.
(12) Szamrej, I.; Janicka, I.; Chrzáscik, I.; Forýs, M. *Radiat. Phys. Chem.* **1989**, *33*, 387.
(13) Quitevis, E. L.; Bowen, K. H.; Liesegange, G. W.; Herschbach, D. R. *J. Phys. Chem.* **1983**, *87*, 2076.
(14) Mark, T. D. *Int. J. Mass Spectrosc. Ion Processes* **1991**, *107*, 143.
(15) Inǵolfsonn, O.; Weik, F.; Illenberger, E. *Int. J. Mass Spectrosc. Ion Processes* **1996**, *155*, 1.
(16) Frisch, M. J.; Trucks, G. W.; Schlegel, H. B.; Gill, P. M. W.; Johnson, B. G.; Robb, M. A.; Cheeseman, J. R.; Keith, T. A.; Petersson, G. A.; Montgomery, J. A.; Raghavachari, K.; Al-Laham, M. A.; Zakrewski, V. G.; Ortiz, J. V.; Foresman, J. B.; Cioslowski, J.; Stefanov, B. B.; Nanayakkara, A.; Challacombe, M.; Peng, C. Y.; Ayala, P. Y.; Chen, W.; Wong, M. W.; Andres, J. L.; Replogle, E. S.; Gomperts, R.; Martin, R. L.; Fox, D. J.; Binkley, J. S.; Defrees, D. J.; Baker, J.; Stewart, J. P.; Head-Gordon, M.; Gonzalez, C.; Pople, J. A. *Gaussian 94, (SGI-Revision B.3)*; Gaussian, Inc.: Pittsburgh, PA, 1995.
(17) Curtiss, L. A.; Raghavachari, K.; Pople, J. A. *J. Chem. Phys.* **1993**, *98*, 1293.
(18) Note that relevant references dealing with the related HCl molecule are included below. For reviews of experimental studies see references (3), (22) and (23).
(19) Taylor, H. S.; Goldstein, E.; Segal, G. A. *J. Phys. B.* **1977**, *10*, 2253.
(20) Krauss, M.; Stevens, W. J. *Chem. Phys.* **1981**, *74*, 570.
(21) O'Neil, S. V.; Rosmus, P.; Norcross, D. W. *J. Chem. Phys.* **1986**, *85*, 7232.
(22) Schwerdtfeger, P.; Szentpaly, L. v.; Stoll, H.; Preuss, H. *J. Chem. Phys.* **1987**, *87*, 510.
(23) Chapman, D. A.; Balasubramanian, K.; Lin, S. H. *Phys. Rev. A.* **1988**, *38*, 6098.
(24) Fandreyer, R.; Burke, P. G.; Morgan, L. A.; Gillan, C. J. *J. Phys. B.* **1993**, *26*, 3625.
(25) (a) Fehsenfeld, F. C.; Howard, C. J.; Ferguson, E. E. *J. Chem. Phys.* **1973**, *58*, 5841. (b) Howard, C. J.; Fehsenfeld, F. C.; McFarland, M. *J. Chem. Phys.* **1974**, *60*, 5086.
(26) DesfranHois, C.; Abdoul-Carime, H.; Khelifa, N.; Scherman, J. P. *Phys. Rev. Lett*. **1994**, *73*, 2436; and references therein.
(27) DesfranHois, C.; Abdoul-Carime, H.; Khelifa, N.; Scherman, J. P. *J. Chem. Phys.* **1995**, *102*, 4952.
(28) See Gutowski, M.; Skurski, P. *J. Chem. Phys.* **1997**, *107*, 2962, and references therein.
(29) Gaussian 98 Manual.
(30) Huber, K. P.; Herzberg, G. *Molecular Spectra and Molecular Structure IV. Constants of Diatomic Molecules*; Van Nostrand: New York, 1979.
(31) Rank, D. H.; Fink, U.; Wiggins, T. A. *J. Mol. Spec.* **1965**, *18*, 170.
(32) Chen, W.; Hight Walker, A. R.; Novick, S. E. *J. Chem. Phys*. **1997**, *106*, 6240.
(33) Latajka, L.; Scheiner, S. *Chem. Phys.* **1997**, *216*, 37.
(34) Barnes, A. J.; Davies, J. B.; Hallam, H. F.; Howells, J. D. R. *J. Chem. Soc., Faraday Trans.* 2 **1973**, *69*, 246.
(35) Hendricks, J. H.; de Clercq, H. L.; Lyapustina, S. A.; Bowen, K. H. *J. Chem. Phys.* **1997**, *107*, 2962.
(36) Ikuta, S.; Saitoh, T.; Nomura, O. *J. Chem. Phys.* **1990**, *93*, 2530.
(37) Del Bene, J. E.; Jordan, M. J. T. *Spectrochim. Acta A* **1999**, *55*, 719.
(38) Milligan, D. E.; Jacox, M. E. *J. Chem. Phys.* **1971**, *55*, 2550.
(39) Caldwell, G.; Kebarle, P. *Can J. Chem.* **1985**, *63*, 1399.
(40) One may recall that $r(H_3{-}Br_4)$ is frozen at this value in the calculation of the surface in Figure 7.
(41) Szamrej, I.; Forýs, M. *Progress in Reaction Kinet.* **1998**, *23*, 117.